Peer-reviewed version available at *Genes* **2019**, *10*, 39; doi:10.3390/genes10010039

Title: **TALEN mediated gene targeting for CF gene therapy**

Emily Xia[1,2,*], Yiqian Zhang [1,2*], Huibi Cao[1], Jun Li[1], Rongqi Duan[1], Jim Hu[1,2,3,**]

[1]Translational Medicine, The Hospital for Sick Children Research Institute, 686 Bay Street, Toronto, Ontario, M5G 0A4, Canada

[2]Department of Laboratory Medicine and Pathobiology and [3]Department of Paediatrics, University of Toronto, 1 King's College Circle, Toronto, Ontario, M5S 1A8, Canada

.

****Corresponding author:** Dr. Jim Hu, Translational Medicine The Hospital for Sick Children Research Institute, Peter Gilgan Centre for Research and Learning (PGCRL), 9th floor, 686 Bay Street, Toronto, ON**.,** Canada, M5G 0A4**,** 416-813-6412 (phone), 416-813-5771 (fax)

***Co-first authors.**

Peer-reviewed version available at Genes 2019, 10, 39; doi:10.3390/genes10010039

ABSTRACT

Cystic Fibrosis (CF) is an inherited monogenic disorder, amenable to gene based therapies. Because CF lung disease is currently the major cause of mortality and morbidity, and lung airway is readily accessible to gene delivery, the major CF gene therapy effort at present is directed to the lung. Although airway epithelial cells are renewed slowly, permanent gene correction through gene editing or targeting in airway stem cells is needed to perpetuate the therapeutic effect. Transcription activator-like effector nuclease (TALEN) has been utilized widely for a variety of gene editing applications. The stringent requirement for nuclease binding target sites allows for gene editing with precision. In this study, we engineered helper-dependent adenoviral (HD-Ad) vectors to deliver a pair of TALENs together with donor DNA targeting the human AAVS1 locus. With homology arms of 4 kb in length, we demonstrated precise insertion of either a *LacZ* reporter gene or a human *CFTR* minigene into the target site. Using the LacZ reporter, we determined the efficiency of gene integration to be about 5%. In the CFTR vector transduced cells, we have detected both CFTR mRNA and protein expression by qPCR and Wetern analysis, respectively. We have also confirmed CFTR function correction by flurometric Image Plate Reader (FLIPR) and iodide efflux assays. Taking together, these findings suggest a new direction for future *in vitro* and *in vivo* studies in CF gene editing.

INTRODUCTION

Cystic Fibrosis (CF) is an inherited autosomal recessive disease most commonly seen in the Caucasian population [1]. CF is caused by mutations in the *cystic fibrosis* transmembrane

conductance regulator (*CFTR*) gene. The most predominant mutation leads to the deletion of phenylalanine residue at position 508 [2]. CF affects multiple organs and currently 80% of mortality is caused by lung failure [3]. Conventional treatments including antibiotics, physical therapy and nutritional supplements can only alleviate the symptoms but does not provide an effective treatment for the disease. Over the past few years, new treatment strategies have been evolving; different types of CFTR channel modulators have been shown to be effective in improving channel activity in CF patients [4][5][6][7][8][9]. Most recently, a triple combinational therapy with VX-440, tezacaftor and ivacaftor has shown significant clinical benefits in an ongoing phase II trial [10]. While substantial progress has been made in the development of CF therapies, current treatment strategies including the multiple channel modulator/corrector usage impose a heavy drug burden on patients. In addition, for a small portion of patients whose mutations lead to no CFTR protein production, there is no effective drug to slow down the disease progression. Furthermore, possibilities of drug interactions may increase the risk of adverse effects [11].

Gene therapy is an attractive strategy for CF lung disease because it treats the underlying cause of the disease rather than its symptoms. Gene replacement therapy for mutations involved in Leber's congenital amaurosis, choroideremia, achromatopsia, and retinitis pigmentosa using AAV vectors has showed correction to various degrees [12][13][14]. Many CF gene therapy trials using adenoviral (Ad) vector, adeno-associated viral (AAV) vector, liposomes as vehicles for delivery have been carried out since early 1990s, but none showed significant improvements in lung function [15][16][17][18]. Nonviral vectors, such as liposomes, in general are not efficient in gene delivery while viral vectors have other problems [19]. For example, AAV vectors have been successfully used in eye gene therapy [13], but it has a small DNA carrying

capacity and thus not suitable for delivering CFTR gene expression cassette. For Ad vectors, one major obstacle is host immune responses elicited by the vectors, which eliminate the vector-transduced cells [20]. To reduce the host immune responses, a helper-depended adenoviral vector (HD-Ad) vector was developed by deleting all viral coding sequences. Thus, this type of vector has a large DNA-carrying capacity up to 36 kb in addition to advantages in reduction of host immune responses [21][22]. Using HD-Ad vectors, our group has demonstrated efficient vector delivery to airway epithelia of mice and pigs with limited immune responses [22][23][24]. More recently, we showed effective delivery of HD-Ad vectors to airway basal cells of mice and pigs [25].

Engineered transcription activator-like effector nucleases (TALENs) are highly efficient in generating double-stranded breaks in cell genomes, which facilitate gene editing via the homology-directed recombination (HDR) process [26]. TALENs bind and cleave their target DNA as heterodimers. Each TALEN monomer is composed of a FokI nuclease fused to a customizable DNA-binding domain [26]. TALEN has been applied in gene editing both *in vitro* and *in vivo* [27][28][28]. Unlike the more popular CRISPR-cas9 system that recognizes a 20 bp target [29], TALEN recognition sequences can be designed longer to provide better specificity and they are commonly designed to be 34 bp in length [30][31].

We have engineered a pair of TALEN that target the human AAVSI locus with assistance from Dr. Bo Zhang group at Peking University, China. Taking the advantage of the large DNA carrying capacity of the HD-Ad vector, we have used it to deliver both TALENs and donor DNA together to target cells at high efficiency. We demonstrate that a LacZ reporter donor gene expression cassette can be successfully integrated into the AAVS1 locus. Furthermore, we have

Peer-reviewed version available at Genes 2019, 10, 39; doi:10.3390/genes10010039

also shown permanent integration of a *CFTR* minigene can be achieved cultured airway epithelial cells. These findings collectively demonstrated feasibility of using TALENs for future targeted *CFTR* gene editing *in vivo*.

RESULT

Co-delivery of TALEN and donor DNA using HD-Ad vectors

The human AAVS1 locus has been extensively explored for targeted gene integration studies as it leads to abundant transgene expression with no adverse consequences [32][33]. To test if large gene constructs, such as the *CFTR* expression cassette [34], can be integrated into this locus, we first tested integration of a LacZ reporter gene expression cassette (Figure 1). For homology-directed gene targeting, homology arms of 4 kb in length were added to either end of the LacZ gene expression cassette (Figure 1A, Supplementary Figure 1). The LacZ HD-Ad vector that harbors both the donor and TALEN genes was produced as described [35]. As shown in Fig. 1B, the transduced human IB3-1 cells showed abundant transgene expression. The TALEN cleavage efficiency was evaluated using the T7E1 assay (Figure 1C). It was around 36% when cells transduced at 50 MOI or 66% when cells transduced at 100 MOI.

Analysis of the LacZ reporter gene integration into the AAVS1 locus

Junction PCR assays indicated precise on-target integration of the LacZ reporter gene into the AAVS1 locus (Figure 2A). Junction PCR products were further subjected to analyses by restriction enzyme (RE) digestion and Sanger sequencing (Figure 2A), both of which further

Peer-reviewed version available at Genes 2019, 10, 39; doi:10.3390/genes10010039

confirmed the identity of junctional PCR products. To evaluate potential off-target cleavage activity of LacZ integration vector, T7E1 assays were performed for the top three potential off-target locations (Figure 2B). Results indicated that there was no detectable off-target activity in transduced cells.

To determine the integration efficiency of LacZ vector, transduced cells were first continuously passaged for 18 generations (Supplementary Figure 2). Passaging was implemented to dilute out residual vector genomes in transduced cells. The LacZ gene integration efficiency was determined by staining for percentage of LacZ-positive cells at passage 18 (Figure 3A,B). The addition of a DNA ligase VI inhibitor, SCR7, has been shown to enhance gene integration by promoting cellular repair via HDR pathway [36]. In line with this finding, we have also observed an increase of 1.5 fold in integration efficiency with SCR7 treatment (Figure 3C). To verify the gene integration efficiency with an independent method, Imagene Green substrate was used to fluorescently label LacZ positive cells at passage 18, and percentage of LacZ positive cells was quantified by flow cytometry (Figure 3D). The integration efficiency determined from LacZ staining was 3% for 50 MOI transduction, 5% for 100 MOI transduction; while flow cytometry showed higher integration efficacy of 6.37% for 50MOI transduction and 8.23% for 100MOI transduction. This discrepancy of integration efficiency seen from two LacZ quantifying methods may have been caused by low level of background substrate reaction since the negative control (NC) from substrate reaction also showed 1.48% of fluorescent cells (Figure 3C).

Integration of *CFTR* gene into the AAVS1 locus allowed persistent CFTR expression and presence of CFTR channel activity.

Peer-reviewed version available at Genes 2019, 10, 39; doi:10.3390/genes10010039

For *CFTR* gene integration, an HD-Ad vector that contains *CFTR* expression cassette [34] flanked by homology arms in addition to TALEN genes was constructed and produced (Figure 4A, Supplementary Figure 1). Following transduction, CFTR protein was expressed in transduced IB3-1 cells (Figure 4A, B, Supplementary Figure 3). Junction PCR on either end of the integration site showed positive products, indicating integration was at the precise location (Figure 4C). PCR product was validated by restriction enzyme digestion and Sanger sequencing (Figure 4C). We further examined *CFTR* mRNA expression at multiple time points after transduction by qPCR, and found that the *CFTR* mRNA level was significantly higher in cells transduced with the integration vector than that in cells transduced with the control (non-integrating) vector (Figure 5A). More importantly, *CFTR* protein was detectable at passage 6 and passage 12 for cells transduced with CFTR integration vector; whereas cells transduced with non-integrating vector failed to show detectable *CFTR* protein expression at passage 12 (Figure 5B).

To assess the level of *CFTR* channel activity, we performed flurometric Image Plate Reader (FLIPR) assays in 96 well-plates with cells treated with *CFTR* integration vector. Results indicated significant *CFTR* channel activity both at initial transduction and at passage 12 (Figure 5C). This result was consistent with CFTR channel activity measured using iodide efflux assay (Supplementary figure 4). Looking at these findings, it is evident that our vector can achieve effective integration of the *CFTR* expression cassette into the AAVS1 locus and allow persistent CFTR expression at mRNA, protein, and functional level.

Transient TALEN expression

Peer-reviewed version available at Genes 2019, 10, 39; doi:10.3390/genes10010039

Because TALEN is a foreign protein and is not naturally expressed in humans, its prolonged expression in hosts may cause unwanted antigenic responses. We therefore examined TALEN expression over time in cells transduced with *CFTR* integration vector. We first monitored the GFP fluorescence level following vector transduced for 12 days and noticed significant decline in GFP fluoresce after day 3 (Figure 6A). We then performed qPCR and Western blotting to measure TALEN expression in transduced cells at multiple time points following integration vector transduction. Results showed that TALEN protein and mRNA expression was undetectable after 5-6 passages (Figure 6B, C, Supplementary Figure 5). In addition, the relative quantity of HD-Ad vector genome measured by qPCR also gradually declined and was undetected after 6 passages (Figure 6B, Supplementary Figure 5). These results collectively indicate that although high level of TALEN expression can be achieved upon initial administration of gene integration vector in cells, its expression was lost gradually in transduced cells. Hence, we conclude that the HD-Ad integration vector does not show prolonged presence of TALEN or vector in transduced cells.

DISCUSSION

In this study we showed insertion of large 8 kb gene constructs into the human AAVS1 locus can be achieved at an efficiency of 5%. Because of the large carrying capacity and high transduction efficiency, both TALEN and donor genes can be simultaneously delivered by a single vector. This method of co-delivery of donor and gene editor cannot be achieved by other viral vectors due to their limited DNA carrying capacity. In addition, our laboratory has also demonstrated that HD-Ad vectors can target the residential progenitor cells in the airway system [25]. This will

Peer-reviewed version available at Genes 2019, 10, 39; doi:10.3390/genes10010039

allow us to explore the possibility of *CFTR* gene editing *in vivo* in progenitor cells for sustained *CFTR* gene expression in the airway system in our future work.

In gene editing studies, one of the crucial safety criteria is the targeting precision. Off-target cleavage at essential genes may cause deleterious consequences. Studies revealed small point mutations such as substitutions and deletions caused by DSB may allow cell transformation into an oncogenic nature [37][38]. The challenge is faced by all the endonuclease-mediated gene editing systems, including, zinc fingers, TALENs and CRISPRs [39]. The CRISPR-cas9 system has been used widely as a versatile tool for gene editing [40]. Compared to the CRISPR-cas9 system which shows off-target effects due to the tolerance for mismatched binding of its short 20 nt recognition sequence [40], TALEN recognition requires a longer binding sequence which minimizes the chance of off-target cleavage [41]. Genome wide off-target studies by looking for cleavage at sequences similar to on-target site revealed lower off-target cleavage for TALEN than for CRISPR-cas9 system [42][43][44][45]. Technical advancements in the field will likely improve the safety profile of all these gene editing systems.

We chose to integrate the *CFTR* expression cassette into the AAVS1 locus, instead of editing a *CFTR* mutation as our strategy for *CFTR* gene correction because this approach is not mutation-specific and it is applicable to correcting all *CFTR* mutations. We selected the AAVS1 locus for the test because it is known that transgenes integrated in this locus can be efficiently expressed. However, future work should consider targeting the *CFTR* locus with this approach since integration of a CFTR expression cassette in the locus can stop the mutant CFTR gene expression. This may be considered an advantage over gene integration into a non-CFTR locus.

The efficiency of site-specific gene integration is important for achieving therapeutic effects in gene therapy. SCR7 treatment has been used previously by other groups to increase CRIPSR-cas9 mediated integration efficiency. We tested different concentrations of SCR7 for its effect on efficiency of gene integration. We did see an increase in integration efficiency on TALEN mediated gene editing although the effect was not as significant as mentioned previously by other groups [36][46]. One reason could be the difference in gene editors utilized as other groups mainly applied SCR7 in combination with the CRISPR-cas9 system. Another reason could be the difference in the cell lines used. We are currently working on enhancing the efficiency of *CFTR* gene integration. We plan to explore the possibility of combining protein factors [47] that facilitate the HDR pathway with TALEN integration vectors.

In this study, we examined the time course of TALEN expression in transduced cells. Since TALEN was derived from a pathogenic bacterial species from plant Xanthomonas (genus)[30], we worry that it may cause antigenic responses in host, which are a significant problem seen in studies of *in vivo* gene therapy [21]. To our favor, this study has shown a rapid clearance of TALEN in the transduced cells, examined at levels of mRNA and protein. This greatly limits the chance of host immune responses that may cause elimination of gene corrected cells. Taking all of these together, our study demonstrated successful TALEN-mediated gene correction in a human *CFTR* mutant cell line as well as rescue of *CFTR* channel activity. This provided new insights in TALEN-mediated gene editing, and opened opportunity for further enhancing the efficiency and performance in future studies.

MATERIAL AND METHODS

Cell culture

IB3-1, a cystic fibrosis cell line derived from human bronchial epithelial cells [48], was maintained in DMEM medium (Life Technologies Canada, Mississauga, ON) containing 10% heat inactivated FBS (Wisent, Saint-Jean-Baptiste, QC) and 100 U/ml penicillin streptomycin (Life Technologies Canada, Mississauga, ON).

Plasmid constructs

TALEN plasmids were generated by Dr. Bo Zhang's lab using the Unit Assembly method [27]. The RVDs HD-HD-HD-HD-NG-HD-HD-NI-HD-HD-HD-HD-NI-HD-NI-NN-NG and NG-NG-NG-HD-NG-NN-NG-HD-NI-HD-HD-NI-NI-NG-HD-HD-NG recognize a region in the AAVS1 site within the human chromosome 19 with a 15-nucleotude spacer. Generation of the UBCLacZ expression cassette was as described in the previously [49]. Left and right homology arms (4kb) were amplified from human cell line A549 (ATCC CCL-185), and cloned into the UBCLacZ vector by in-fushion cloning (Clontech). The UBCLacZ expression cassette with homology arms was cloned into an HD-Ad backbone plasmid pC4HSU (NotI/SalI)[50]. The PmeI sites on the resulting vectors were switched to PacI sites using infusion cloning. The assembled UBCLacZ plasmid pC4HSU-UBCLacZ-L4-R4 was linearized with NheI followed by blunt end treatment with T4 DNA polymerase (New England Biolabs, Whitby, ON), then digested with NsiI. The DNA fragment for TALEN expression was cleaved and ligated using FspI and Nsilsites. The resulting vectors were denominated as pHD-Ad-UBCLacZ-TALEN.

Peer-reviewed version available at Genes 2019, 10, 39; doi:10.3390/genes10010039

The same methods as described above were used to add the 4 kb homology arms to the K18CFTR expression cassette carried by pBSII-SK(+) backbone plasmid. Similarly, the expression cassette and the homology arms were cloned into pC4HSU backbone (NotI/SalI). The DNA fragment for TALEN expression was inserted to the pC4HSU-K18CFTR-L4-R4 by AscI digestion and ligation. The resulting plasmid was denominated as pHD-Ad-K18CFTR-TALEN.

Vector production

HD-Ad-UBCLacZ-TALEN and HD-Ad-K18CFTR-TALEN vectors were produced as previously described [35]. Briefly, HD-Ad vectors were packaged by transfecting 116 producer cells with the linearized pHD-Ad vector and tansduced with NG163 helper virus. In 116 cells, HD-Ad vectors were amplified by serial passage and then purified by CsCl density gradient ultracentrifugation. Viral particle numbers of HD-Ad preparations were determined by spectrophotometry.

Transduction

IB3-1 cells were seeded in 6-well dishes and cultured until 70% confluency. Before transduction, cells were washed with pre-warmed PBS, pH 7.4. HD-Ad vectors were added to the cells at 50 MOI and 100 MOI in 0.5 mL of serum-free media. Cells were incubated for 1 hour before adding pre-warmed media to make a final volume of 2 ml per well. Transduced IB3-1 cells were cultured for 5 days before the first passage. After the first passage, the cells were split twice per week at a ratio of 1:7.

Measurement of cleavage efficiency

Peer-reviewed version available at Genes 2019, 10, 39; doi:10.3390/genes10010039

Cells were collected and lysed using the Genomic Cleavage Detection Kit (thermofisher, Waltham, MA) 72 h post-transduction. A 644 bp region covering the TALEN target site was amplified; 5' GAT CCT CTC TGG CTC CAT CGT AAG CAA AC 3' (forward primer) and 5' GAT GGC CTT CTC CGA CGG ATG TCT C 3' (reverse primer). The PCR products were denatured at 95°C for 5 min, followed by re-annealing at a ramp rate of -2°C/s from 95-85°C and -0.1°C/s from 85-25°C. The T7 enzyme was added and the mixtures were incubated at 37°C for 30 min before the reactions were terminated by adding 1.5 µL of 0.25 M EDTA. Resulted DNA bands were visualized on a 2% agarose gel. The band intensities were analyzed with ImageJ.

Off-target analysis

Top 3 off-target sites in the human genome were predicted by the TALEN offer programme (http://galaxy.informatik.uni-halle.de/root?tool_id=TALENoffer). PCR primers were designed to amplify regions around the predicted sites. Primers sequences and the corresponding length of the amplicons are: 5' GTA CAG CAA TCT AAG GAA GTA GAC TCT TAG G 3' (forward primer) and 5' GTT TCA CTA TGT TGG TCA GGC TGC TC 3' (reverse primer) for off-target site #1 (738 bp), 5' GTC TGA TTG TGC AGG TTG TGT AGG ATC 3' (forward primer) and 5' CAC CCA AGT GCT GAC CTT ACT GC 3' (reverse primer) for off-target site #2 (687 bp), and 5' CAG CAG TCA GGG TTG TTC AGT TTG TTC 3' (forward primer) and 5' CCT AAA CCT TGG TGG CTA AAC ACA GTA AAA G 3' (reverse primer) for off-target site #3 (763 bp). PCR products at the three selected sites were then analyzed using T7E1 assays as described in the previous section.

Verification of on-target integration

Genomic DNA of cells were collected 5-day post-transduction. Junction PCR was performed on a SimpliAmp Thermal Cycler (Applied Biosystems, Foster city, CA). The sequences of primer sets used and the size of amplicons are as follows: UBCLacZ left junction, 4.5 kb amplicon, 5' CAT CAG CGA TGC AAT GAT GCT TGG GTT TGC ACC AAT G 3' (forward primer), 5' TCC TTC TGC TGA TAC TGG GGT TCT AAG GCC GAG TC 3' (reverse primer); UBCLacZ right junction, 4.4 kb amplicon, 5' GGT TTT TCA CAG ACC GCT TTC TAA GG 3' (forward primer), 5' GTT GGA GGA GGA AGG AGA CAG AAT CC 3' (reverse primer). K18CFTR left junction, 4.6 kb amplicon, 5' CAT CAG CGA TGC AAT GAT GCT TGG GTT TGC ACC AAT G 3' (forward primer), 5' GGC AGA GCA CAG ATA AAG AGC CTG AGC CTG GAT TG 3' (reverse primer); K18CFTR right junction, 4.7 kb amplicon, 5' GAA TTC GAT GTG CTG GGA TCA GGA G 3' (forward primer), 5' GTT GGA GGA GGA AGG AGA CAG AAT CC 3' (reverse primer). PCR products were purified and digested with EcoRV or AfeI. Sanger sequencing was performed by the Centre for Applied Genomics at the Hospital for Sick Children.

SCR7 treatment

The NHEJ inhibitor SCR7 (Xcess Biosciences, San Diego, CA) was added at 0.1 and 0.5 μM directly to IB3-1 cells transduced with HD-Ad-UBCLacZ-TALEN 20 hours post-transduction. Treated cells were cultured until day 5 after the transduction and passaged as normal.

β-galactosidase staining for integration efficiency

Transduced IB3-1 cells were washed with PBS, pH 8.0 and fixed in 0.5% glutaraldehyde in PBS for 15 min. After PBS washing, β-galactosidase staining solution (0.1% X-gal, 2 mM $MgCl_2$, 5

Peer-reviewed version available at Genes 2019, 10, 39; doi:10.3390/genes10010039

mM K-ferricyanide, 5 mM K-ferrocyanide in PBS) was added to cover the cell monolayer. Cells were incubated at 37°C overnight in dark. To terminate the reaction, the staining solution was removed from the dish and the cells were washed with PBS.

To monitor the transduction efficiency, IB3-1 cells were stained 3 days post-transduction. To assess the integration efficiency, IB3-1 cells were passed for 18 passages before staining. Twenty images were taken randomly for each well under a bright field microscope at 100x magnification. The number of LacZ positive cells and the total number of cells in each image were recorded with ImageJ. The transduction and integration efficiencies were calculated according to the following formulas: % transduction = 100 x sum of LacZ positive cells from all 20 images / sum of total number of cells from all 20 images; % integration = 100 x sum of LacZ positive cells from all 20 images / (sum of total number of cells from all 20 images x transduction efficiency).

Single cell colonies

Transduced IB3-1 cells were cultured for 12 passages before single cell sorting. Upon 70% confluency, the cells were suspended in ice-cold PBS, pH 7.4 containing 1% FBS. The cells were incubated on ice in the dark with 7-AAD (BioLegend, San Diego, CA) at a concentration of 100 ng per million cells for 10 minutes. Single cells were sorted directly into 96-well plates containing 20% DMEM medium supplemented with 20% FBS (MoFloXDP BRV/UV). Sorted cells were cultured for 2 weeks until assaying.

Flow cytometry

Peer-reviewed version available at Genes 2019, 10, 39; doi:10.3390/genes10010039

Upon 90% confluency, transduced IB3-1 cells at passage 18 were gently washed with PBS, pH 7.4, scraped from the plates in 1 mL of PBS, and spun down at 400 rpm for 1 minute at room temperature. cell pellet was resuspended in 300 µLof DMEM, high glucose, HEPES, no phenol red (Life Technologies Canada, Mississauga, ON) with 3 microliter of 30 mM chloroquine diphosphate and incubated at 37°C for 30 minutes. 3.3 µL of 1:10 diluted ImaGene Green C_{12}FDG substrate reagent (Invitrogen, Waltham, MA) was added and samples were incubated 37°C for 45 minutes in dark. Then, cells were washed and suspended in 500 microliter of media containing 500uM of phenyl-ethyl β-D-thiogalactopyranoside (PETG) (Invitrogen, Waltham, MA) and 7-AAD. Afterwards, cells were filtered and analyzed on LSRII-CFI, VBGR 15-colour analyzer (Becton Dickinson, Missisauga, ON). Flow cytometry data were analyzed using flowjo.

RNA isolation and quantitative RT-PCR

Total RNA from IB3-1 cells transduced with HD-Ad-K18CFTR-TALEN or the control vector at 100 MOI were harvested and purified with the PureLink RNA Mini Kit (Life Technologies, Waltham, MA) following the manufacturer's instructions at 3 days, 6 passages, 12 passages, and 18 passages post-transduction, followed by DNase I digestion at room temperature for 15 minutes. One microgram of total RNA was reverse-transcribed using SuperScript VILO Master Mix (Invitrogen, Waltham, MA) according to the manufacturer's protocol. Ten nanograms of cDNA samples were loaded as templates for real-time PCR using Power SYBR Green PCR Master Mix on a QuantStudio 3 Thermal Cycler (Applied Biosystems, Foster city, CA). The primers for detecting human CFTR cDNA are 5' CCT GAG TCC TGT CCT TTC TC 3' (forward primer) and 5' CGC TGT CTG TAT CCT TTC CTC 3' (reverse primer). GAPDH

Peer-reviewed version available at Genes 2019, 10, 39; doi:10.3390/genes10010039

cDNA were measured as the internal control using primers 5' GTT CGA CAG ACA GCC GTG TG 3' (forward primer) and 5' ATG GCG ACA ATG TCC ACT TTG C 3' (reverse primer). Relative hCFTR mRNA expression was calculated as expression = $2^{-\Delta\Delta CT}$.

CFTR Immunofluorescence

IB3-1 cells were seeded onto collagen-coated round glass cover slips in 6-well plates 3 days prior to staining. At confluency, cells were washed in PBS, pH 7.4, fixed in ice-cold methanol for 10 minutes, and permeabilized with 0.5% Triton-100 in PBS. Cells were then blocked for 1 hour in block solution (5% goat serum, 0.5% BSA, 0.05% Triton-100 in PBS). Cells were incubated with mouse monoclonal antibodies against the human *CFTR* R-domain MAB1660 and C-terminus MAB25031 (R&D Systems, Minneapolis, MN) at 1:500 dilution overnight at 4°C, washed in PBS with 0.05% Triton-100, and then incubated in dark for 1 hour in 1:750 diluted CF555 goat anti-mouse IgG (H+L) (Biotium, Fremount, CA). After washes in dark, cells on the glass slips were taken out from the 6-well plates, and mounted with one drop of VECTASHIELD HardSet Antifade Mounting Medium with DAPI (Vector Laboratories, Burlington, ON).

Protein isolation and CFTR Immunoblot

IB3-1 cells were gently washed with ice-cold PBS, pH 7.4 then scraped from the bottom of the plate with a cell scraper in 1 mL of ice-cold PBS and centrifuged at 4°C. Cell pellet was re-suspended on ice in 30 µL of RIPA buffer (1% Triton X-100, 0.1% SDS, 150 mMNaCl, 20 mMTrisHCl, and 0.5% sodium deoxycholate) supplemented with cOmplete Protease Inhibitor Cocktail (Roche, Mississauga, ON). The cells were lysed on ice with occasional vortex, then

centrifuged at 4°C. Protein samples were denatured with one volume of 4x Laemmli protein sample buffer for SDS-PAGE (Bio-Rad, Mississauga, ON).

Protein samples were loaded onto polyacrylamide gel at 100 µL per lane and run at 100 volts for 90 minutes. The proteins in the gel were transferred onto a piece of nitrocellulose membrane at 85 V for 90 minutes on ice. The membrane was blocked in 5% skim milk in TBS-T (0.1% Tween 20 in TBS, pH 7.4) at room temperature with shaking, then incubated in 1:1000 diluted primary mouse anti-*CFTR* antibody MAB 596 (University of North Carolina) or 1:2000 diluted primary rabbit anti-GAPDH antibody ab9485 (Abcam, San Francisco, CA) overnight at 4°C. On the next day, membranes were washed with TBS-T and incubated with 1:3000 diluted secondary antibodies(Bio-Rad). The membranes were treated with Western Lightning Plus-ECL Solutions (PerkinElmer, Woodbridge, ON) and protein bands were visualized with ChemiDoc XRS+ (Bio-Rad, Mississauga, ON).

Protein analysis with automated western system-JESS

Total protein isolation was carried out as described in the previous section. Protein samples (1mg) were mixed with 5X fluorescence detection master mix before loading onto each of the capillary reaction chamber. For CFTR protein detection, five microliter of 1:400 diluted anti-mouse CFTR antibody (MAB 596, University of North Carolina) and 5 µl of 1:400 diluted anti-rabbit GAPDH antibody (ab9485, Abcam) were used for each lane. For TALEN protein detection, 5 microliters of 1:400 diluted mouse-anti-flag antibody and 5µl of 1:400 diluted anti-rabbit GAPDH antibody (ab9485, Abcam) were used for each lane. Ten microliters of combined secondary anti-M and anti-R rabbit antibody were used for each sample. The whole analysis including protein

Peer-reviewed version available at Genes 2019, 10, 39; doi:10.3390/genes10010039

separation, primary and secondary antibody probing, and chemi-fluorescence detection, was done automatically by the JESS system (ProteinSimple, San Jose, CA) under 5 hours. Results from 24 samples were displayed and analyzed using the Compass analysis software.

Membrane potential assay

Protocol for membrane potential assay was adapted from Ahmadi *et al* [51]. Cells were seeded to black-walled, clear-bottom 96-well plates and cultured until 100% confluency. The blue membrane potential dye (Molecular Devices) was dissolved in a chloride-free buffer (150 mM NMDG-gluconate, 3 mMKCl, 10 mM HEPES, pH 7.35, osmolarity 300 mOsm) and loaded to the cells. The plates were incubated at 37°C with 5% CO_2 and humidified air for 30 minutes, then transferred to the i3 multi-well microplate reader (Molecular Devices, San Jose, CA). Eleven baseline reads were made, followed by addition of 2.5 µL forskolin per well. After adding the drug, 31 reads were made. Then, 21 scans were made after the reaction was terminated by addition of 10 µM CFTRinh-172. For negative controls, 2.5 microliter of DMSO was added instead of forskolin.

Statistical analysis

Unpaired student's t-test was used for the comparison between means of two groups. A p value less than 0.05 was considered statistically significant. Error bars were shown in standard error of the mean (SEM).

Acknowledgements:

We would like to thank Dr. Bo Zhang and her lab members at Peking University, Beijing, China for designing and generating all TALEN plasmids used in this study. We thank Ms. Sara Chowns for reading and commenting on the manuscript. This study was funded by Canadian Institute for Health Research (CIHR) grants (MOP 125882), Cystic Fibrosis Foundation Therapeutics, Inc. grant (HU15XX0) and Cystic Fibrosis Canada grant (#3032) to JH.

REFERENCE

[1] Spoonhower KA, Davis PB. Epidemiology of Cystic Fibrosis. Clin Chest Med 2016. doi:10.1016/j.ccm.2015.10.002.

[2] Cutting GR. Cystic fibrosis genetics: from molecular understanding to clinical application. Nat Rev Genet 2014;16:45–56. doi:10.1038/nrg3849.

[3] Martin C, Hamard C, Kanaan R, Boussaud V, Grenet D, Abély M, et al. Causes of death in French cystic fibrosis patients: The need for improvement in transplantation referral strategies! J Cyst Fibros 2016. doi:10.1016/j.jcf.2015.09.002.

[4] De Boeck K, Munck A, Walker S, Faro A, Hiatt P, Gilmartin G, et al. Efficacy and safety of ivacaftor in patients with cystic fibrosis and a non-G551D gating mutation. J Cyst Fibros 2014. doi:10.1016/j.jcf.2014.09.005.

[5] Sermet-Gaudelus I. Ivacaftor treatment in patients with cystic fibrosis and the G551D-CFTR mutation. Eur Respir Rev 2013. doi:10.1183/09059180.00008512.

[6] Flume PA, Liou TG, Borowitz DS, Li H, Yen K, Ordoñez CL, et al. Ivacaftor in subjects with cystic fibrosis who are homozygous for the F508del-CFTR mutation. Chest 2012. doi:10.1378/chest.11-2672.

[7] Milla CE, Ratjen F, Marigowda G, Liu F, Waltz D, Rosenfeld M. Lumacaftor/Ivacaftor in patients aged 6-11 years with cystic fibrosis and homozygous for F508del-CFTR. Am J Respir Crit Care Med 2017. doi:10.1164/rccm.201608-1754OC.

[8] Accurso FJ, Rowe SM, Clancy JP, Boyle MP, Dunitz JM, Durie PR, et al. Effect of VX-770 in Persons with Cystic Fibrosis and the G551D- *CFTR* Mutation. N Engl J Med 2010. doi:10.1056/NEJMoa0909825.

[9] Kopeikin Z, Yuksek Z, Yang HY, Bompadre SG. Combined effects of VX-770 and VX-809 on several functional abnormalities of F508del-CFTR channels. J Cyst Fibros 2014. doi:10.1016/j.jcf.2014.04.003.

[10] Davies JC, Colombo C, Tullis E, Mckee C, Desouza C, Waltz D, et al. WS01.6 Preliminary safety and efficacy of triple combination CFTR modulator regimens in cystic fibrosis. J Cyst Fibros 2018;17:S3. doi:10.1016/S1569-1993(18)30124-3.

[11] Fajac I, De Boeck K. New horizons for cystic fibrosis treatment. Pharmacol Ther 2017. doi:10.1016/j.pharmthera.2016.11.009.

[12] Simonelli F, Maguire AM, Testa F, Pierce EA, Mingozzi F, Bennicelli JL, et al. Gene therapy for leber's congenital amaurosis is safe and effective through 1.5 years after vector administration. Mol Ther 2010;18:643–50. doi:10.1038/mt.2009.277.

[13] MacLaren RE, Groppe M, Barnard AR, Cottriall CL, Tolmachova T, Seymour L, et al. Retinal gene therapy in patients with choroideremia: initial findings from a phase 1/2 clinical trial. Lancet (London, England) 2014. doi:10.1016/S0140-6736(13)62117-0.

[14] Ghazi NG, Abboud EB, Nowilaty SR, Alkuraya H, Alhommadi A, Cai H, et al. Treatment of retinitis pigmentosa due to MERTK mutations by ocular subretinal injection of adeno-

associated virus gene vector: results of a phase I trial. Hum Genet 2016. doi:10.1007/s00439-016-1637-y.

[15] Moss RB, Milla C, Colombo J, Accurso F, Zeitlin PL, Clancy JP, et al. Repeated Aerosolized AAV-CFTR for Treatment of Cystic Fibrosis: A Randomized Placebo-Controlled Phase 2B Trial. Hum Gene Ther 2007. doi:10.1089/hum.2007.022.

[16] Moss RB, Rodman D, Spencer LT, Aitken ML, Zeitlin PL, Waltz D, et al. Repeated adeno-associated virus serotype 2 aerosol-mediated cystic fibrosis transmembrane regulator gene transfer to the lungs of patients with cystic fibrosis: a multicenter, double-blind, placebo-controlled trial. Chest 2004. doi:10.1378/chest.125.2.509.

[17] Knowles MR, Hohneker KW, Zhou Z, Olsen JC, Noah TL, Hu PC, et al. A controlled study of adenoviral-vector-mediated gene transfer in the nasal epithelium of patients with cystic fibrosis. N Engl J Med 1995;333:823–31. doi:10.1056/NEJM199509283331302.

[18] Alton EWFW, Armstrong DK, Ashby D, Bayfield KJ, Bilton D, Bloomfield E V., et al. Repeated nebulisation of non-viral CFTR gene therapy in patients with cystic fibrosis: A randomised, double-blind, placebo-controlled, phase 2b trial. Lancet Respir Med 2015. doi:10.1016/S2213-2600(15)00245-3.

[19] Xia E, Munegowda MA, Cao H, Hu J. Lung gene therapy-How to capture illumination from the light already present in the tunnel. Genes Dis 2014;1:40–52. doi:10.1016/j.gendis.2014.06.001.

[20] Cao H, Koehler DR, Hu J. Adenoviral Vectors for Gene Replacement Therapy. VIRAL Immunol 2004;17:327–33. doi:10.1089/vim.2004.17.327.

[21] Vetrini F, Ng P. Gene therapy with helper-dependent adenoviral vectors: Current

advances and future perspectives. Viruses 2010. doi:10.3390/v2091886.

[22] Koehler DR, Sajjan U, Chow Y-H, Martin B, Kent G, Tanswell AK, et al. Protection of Cftr knockout mice from acute lung infection by a helper-dependent adenoviral vector expressing Cftr in airway epithelia. Proc Natl Acad Sci U S A 2003;100:15364–9. doi:10.1073/pnas.2436478100.

[23] Toietta G, Koehler DR, Finegold MJ, Lee B, Hu J, Beaudet AL. Reduced inflammation and improved airway expression using helper-dependent adenoviral vectors with a K18 promoter. Mol Ther 2003. doi:10.1016/S1525-0016(03)00059-5.

[24] Cao H, Machuca TN, Yeung JC, Wu J, Du K, Duan C, et al. Efficient gene delivery to pig airway epithelia and submucosal glands using helper-dependent adenoviral vectors. Mol Ther - Nucleic Acids 2013. doi:10.1038/mtna.2013.55.

[25] Cao H, Ouyang H, Grasemann H, Bartlett C, Du K, Duan R, et al. Transducing airway basal cells with a helper-dependent adenoviral vector for lung gene therapy. Hum Gene Ther 2018;6412:hum.2017.201. doi:10.1089/hum.2017.201.

[26] Miller JC, Tan S, Qiao G, Barlow KA, Wang J, Xia DF, et al. A TALE nuclease architecture for efficient genome editing. Nat Biotechnol 2011. doi:10.1038/nbt.1755.

[27] SHEN Y, XIAO A, HUANG P, WANG W-Y, ZHU Z-Y, ZHANG B. TALE nuclease engineering and targeted genome modification. Hered 2013. doi:10.3724/SP.J.1005.2013.00395.

[28] Carlson DF, Tan W, Lillico SG, Stverakova D, Proudfoot C, Christian M, et al. Efficient TALEN-mediated gene knockout in livestock. Proc Natl Acad Sci 2012. doi:10.1073/pnas.1211446109.

[29] Cong L, Ran FA, Cox D, Lin S, Barretto R, Habib N, et al. Multiplex genome engineering using CRISPR/Cas systems. Science 2013;339:819–23. doi:10.1126/science.1231143.

[30] Ding Q, Lee YK, Schaefer EAK, Peters DT, Veres A, Kim K, et al. A TALEN genome-editing system for generating human stem cell-based disease models. Cell Stem Cell 2013. doi:10.1016/j.stem.2012.11.011.

[31] Mussolino C, Alzubi J, Fine EJ, Morbitzer R, Cradick TJ, Lahaye T, et al. TALENs facilitate targeted genome editing in human cells with high specificity and low cytotoxicity. Nucleic Acids Res 2014. doi:10.1093/nar/gku305.

[32] S.S. DR, A. R, P.-Q. L, L. L, M.V. P, N. T, et al. Genome editing of primary human CD34+ hematopoietic stem cells enables a safe harbor targeted gene addition therapeutic strategy for chronic granulomatous disease. Mol Ther 2015.

[33] Smith JR, Maguire S, Davis LA, Alexander M, Yang F, Chandran S, et al. Robust, Persistent Transgene Expression in Human Embryonic Stem Cells Is Achieved with AAVS1-Targeted Integration. Stem Cells 2008. doi:10.1634/stemcells.2007-0039.

[34] Chow YH, O'Brodovich H, Plumb J, Wen Y, Sohn KJ, Lu Z, et al. Development of an epithelium-specific expression cassette with human DNA regulatory elements for transgene expression in lung airways. Proc Natl Acad Sci U S A 1997. doi:10.1073/pnas.94.26.14695.

[35] Palmer DJ, Ng P. Methods for the production of helper-dependent adenoviral vectors. Methods Mol Biol 2008;433:33–53. doi:10.1007/978-1-59745-237-3_3.

[36] Maruyama T, Dougan SK, Truttmann MC, Bilate AM, Ingram JR, Ploegh HL. Increasing the efficiency of precise genome editing with CRISPR-Cas9 by inhibition of

nonhomologous end joining. Nat Biotechnol 2015. doi:10.1038/nbt.3190.

[37] Andersson DI, Hughes D. Antibiotic resistance and its cost: Is it possible to reverse resistance? Nat Rev Microbiol 2010. doi:10.1038/nrmicro2319.

[38] Watson IR, Takahashi K, Futreal PA, Chin L. Emerging patterns of somatic mutations in cancer. Nat Rev Genet 2013. doi:10.1038/nrg3539.

[39] Gaj T, Gersbach CA, Barbas CF. ZFN, TALEN, and CRISPR/Cas-based methods for genome engineering. Trends Biotechnol 2013. doi:10.1016/j.tibtech.2013.04.004.

[40] Chavez A, Pruitt BW, Tuttle M, Shapiro RS, Cecchi RJ, Winston J, et al. Precise Cas9 targeting enables genomic mutation prevention. Proc Natl Acad Sci 2018. doi:10.1073/pnas.1718148115.

[41] Guilinger JP, Pattanayak V, Reyon D, Tsai SQ, Sander JD, Joung JK, et al. Broad specificity profiling of TALENs results in engineered nucleases with improved DNA-cleavage specificity. Nat Methods 2014. doi:10.1038/nmeth.2845.

[42] Hockemeyer D, Wang H, Kiani S, Lai CS, Gao Q, Cassady JP, et al. Genetic engineering of human pluripotent cells using TALE nucleases. Nat Biotechnol 2011. doi:10.1038/nbt.1927.

[43] Mussolino C, Morbitzer R, Lütge F, Dannemann N, Lahaye T, Cathomen T. A novel TALE nuclease scaffold enables high genome editing activity in combination with low toxicity. Nucleic Acids Res 2011. doi:10.1093/nar/gkr597.

[44] Fu Y, Foden JA, Khayter C, Maeder ML, Reyon D, Joung JK, et al. High-frequency off-target mutagenesis induced by CRISPR-Cas nucleases in human cells. Nat Biotechnol 2013. doi:10.1038/nbt.2623.

[45] Hsu PD, Scott DA, Weinstein JA, Ran FA, Konermann S, Agarwala V, et al. DNA targeting specificity of RNA-guided Cas9 nucleases. Nat Biotechnol 2013. doi:10.1038/nbt.2647.

[46] Li G, Zhang X, Zhong C, Mo J, Quan R, Yang J, et al. Small molecules enhance CRISPR/Cas9-mediated homology-directed genome editing in primary cells. Sci Rep 2017;7. doi:10.1038/s41598-017-09306-x.

[47] Canny MD, Moatti N, Wan LCK, Fradet-Turcotte A, Krasner D, Mateos-Gomez PA, et al. Inhibition of 53BP1 favors homology-dependent DNA repair and increases CRISPR-Cas9 genome-editing efficiency. Nat Biotechnol 2018;36:95–102. doi:10.1038/nbt.4021.

[48] Zeitlin PL, Lu L, Rhim J, Cutting G, Stetten G, Kieffer KA, et al. A cystic fibrosis bronchial epithelial cell line: immortalization by adeno-12-SV40 infection. Am J Respir Cell Mol Biol 1991;4:313–9. doi:10.1165/ajrcmb/4.4.313.

[49] Koehler DR, Chow YH, Plumb J, Wen Y, Rafii B, Belcastro R, et al. A human epithelium-specific vector optimized in rat pneumocytes for lung gene therapy. Pediatr Res 2000;48:184–90. doi:10.1203/00006450-200008000-00011.

[50] Sandig V, Youil R, Bett AJ, Franlin LL, Oshima M, Maione D, et al. Optimization of the helper-dependent adenovirus system for production and potency in vivo. Proc Natl Acad Sci U S A 2000;97:1002–7. doi:10.1073/pnas.97.3.1002.

[51] Ahmadi S, Bozoky Z, Di Paola M, Xia S, Li C, Wong AP, et al. Phenotypic profiling of CFTR modulators in patient-derived respiratory epithelia. Npj Genomic Med 2017. doi:10.1038/s41525-017-0015-6.

Figure legend:

Figure 1. Co-delivery of TALENs and donor DNA using HD-AD vectors. A. Schematic representation of HD-Ad vector-mediated integration of a gene cassette for expressing the LacZ reporter or human *CFTR* into Exon 2 of AAVSI locus. B. Transduction of IB3-1 cells with a negative control (HD-Ad-K18LacZ) vector at 100 MOI and HD-Ad-UBCLacZ-TALEN vector at 50 and 100 MOI. GFP fluorescence (conjugated to TALEN) indicates TALEN expression while X-gal staining detects cells with LacZ expression. C. T7E1 assay for assessing the cleavage efficiency of cells transduced with the HD-Ad-K18LacZ-TALEN vector. Human IB3-1 cells were transduced with the vector at 50 MOI (Lane 2,5) and 100MOI (Lane 3, 6). Cells transduced with 100 MOI of HD-Ad-K18LacZ (Lane 1, 4) were used as negative controls. Lanes 1-3 were samples with T7 endonuclease treatment while Lanes 4-6 were samples with no T7 endonuclease treatment. The arrow indicates the uncut PCR product.

Figure 2. Characterization of site-specific gene integration. A. Identification of the integration site by junction PCR. Left: correct integration indicated by positive junction PCR product of 4.5 kb (left side junction, lane 1) and 4.4 kb (right side junction, lane 2). Lanes 3, 4 are left and right side junction PCR assessment of IB3-1 cells transduced with 100 MOI of HD-Ad-UBCLacZ control vector. Middle: Restriction enzyme digestion of junction PCR products. Lane 1, left side junction PCR product digested with EcoRV; Lane 2, left side junction PCR product digested with AfeI; Lane 3, right side junction PCR product digested with EcoRV; Lane 4, right side junction PCR product digested with AfeI. Right: Sanger sequencing of junction PCR products. B. Off-target analysis for TALEN integration vector. Top 3 potential off-target sites were provided using TALENoffer (http://galaxy.informatik.uni-halle.de/root?tool_id=TALENoffer). T7E1 assays for IB3-1 cells transduced with 100MOI of HD-Ad-UBClacZ-TALEN vector were

performed to detect off-target cleavage activity. Arrows indicate positions of the potential off-target cleavage products. The potential off-target sequences are listed at the bottom.

Figure 3. Analysis of the integration efficiency with the HD-Ad-UBCLacZ-TALEN vector. A. X-gal staining for IB3-1 cells transduced with 100MOI of HD-Ad-UBCLacZ-TALEN or HD-Ad-UBCLacZ at passage 18. B. Quantification of integration efficiency of cells transduced with 50 MOI or 100 MOI of HD-Ad-UBCLacZ-TALEN; NC, IB3-1 cells transduced with HD-Ad-UBCLacZ vector at 100 MOI. N=3; *$p<0.05$, ****$p<0.0001$. C. Integration efficiency of HD-Ad-UBCLacZ-TALEN in cells treated with different concentrations of SCR7. **$p<0.01$; n.s., $p>0.5$. D. Flow cytometry quantification of LacZ positive cells. IB3-1 cells transduced with 50MOI or 100MOI of HD-Ad-UBCLacZ-TALEN vector or 100MOI of UBCLacZ vector were passaged for 18 generations and stained with Imagene green LacZ staining dye. Percentages of LacZ positive cells were shown on the FITC vs. FSC plot.

Figure 4. Integration of the human CFTR gene expression cassette into the AAVS1 locus. A. fluorescent images of IB3-1 cells transduced with 50MOI or 100MOI of HD-Ad-K18CFTR-TALEN vector; NC, untransduced cells. B. Western blot for CFTR protein from cell lysate isolated 3 days post-transduction of 100MOI of HD-Ad-K18CFTR-TALEN vector. C. Validation of the site-specific integration. Left panel, junction PCR analysis for IB3-1 cells transduced with HD-Ad-K18CFTR-TALEN vector. Lane 1 shows the 4.6 kb product from left side junction and lane 2 shows the 4.7 kb product from right side junction. Lanes 3 and 4 are negative control PCR reaction for left and right side junction, respectively. Middle panel, restriction analysis of the junctional PCR products. Lane 1 and 2 are left side junction PCR product digested with EcoRV and AfeI, respectively; Lane 3 and 4 are right side junction PCR

product digested with EcoRV and AfeI, respectively. Right panel, Sanger sequencing around junction site of the PCR products.

Figure 5. Analysis of CFTR mRNA and protein expression, and channel function. A. qPCR quantification of CFTR mRNA expression from IB3-1 cells transduced with 100 MOI of HD-Ad-K18CFTR-TALEN vector compared to the control vector (without TALEN) at different passages. *$p<0.05$. B. CFTR western performed using the JESS system. IB3-1 cells were transduced with 100 MOI of HD-Ad-K18CFTR-TALEN vector or 100 MOI of HD-Ad-K18CFTR vector. Lysates were collected at passage 0, passage 6, and passage 12. C. CFTR channel function was measured by FLIPR assay of IB3-1 cells transduced with 100 MOI of HD-Ad-K18-CFTR-TALEN vector, HD-Ad-K18LacZ TALEN vector, and untransduced cells.

Figure 6. Disappearance of TALEN expression and vector genome over time. A. GFP fluorescence at different time points following HD-Ad-K18CFTR-TALEN vector transduction 100 MOI. B. qPCR quantification of TALEN mRNA levels as well as vector genome in IB3-1 cells transduced with Hd-Ad-K18CFTR-TALEN vector. C. Western blot analysis of TALEN protein expression at different time points post transduction using the JESS system.

Preprints (www.preprints.org) | NOT PEER-REVIEWED | Posted: 19 November 2018 doi:10.20944/preprints201811.0444.v1

Peer-reviewed version available at Genes 2019, 10, 39; doi:10.3390/genes10010039

Figure 1

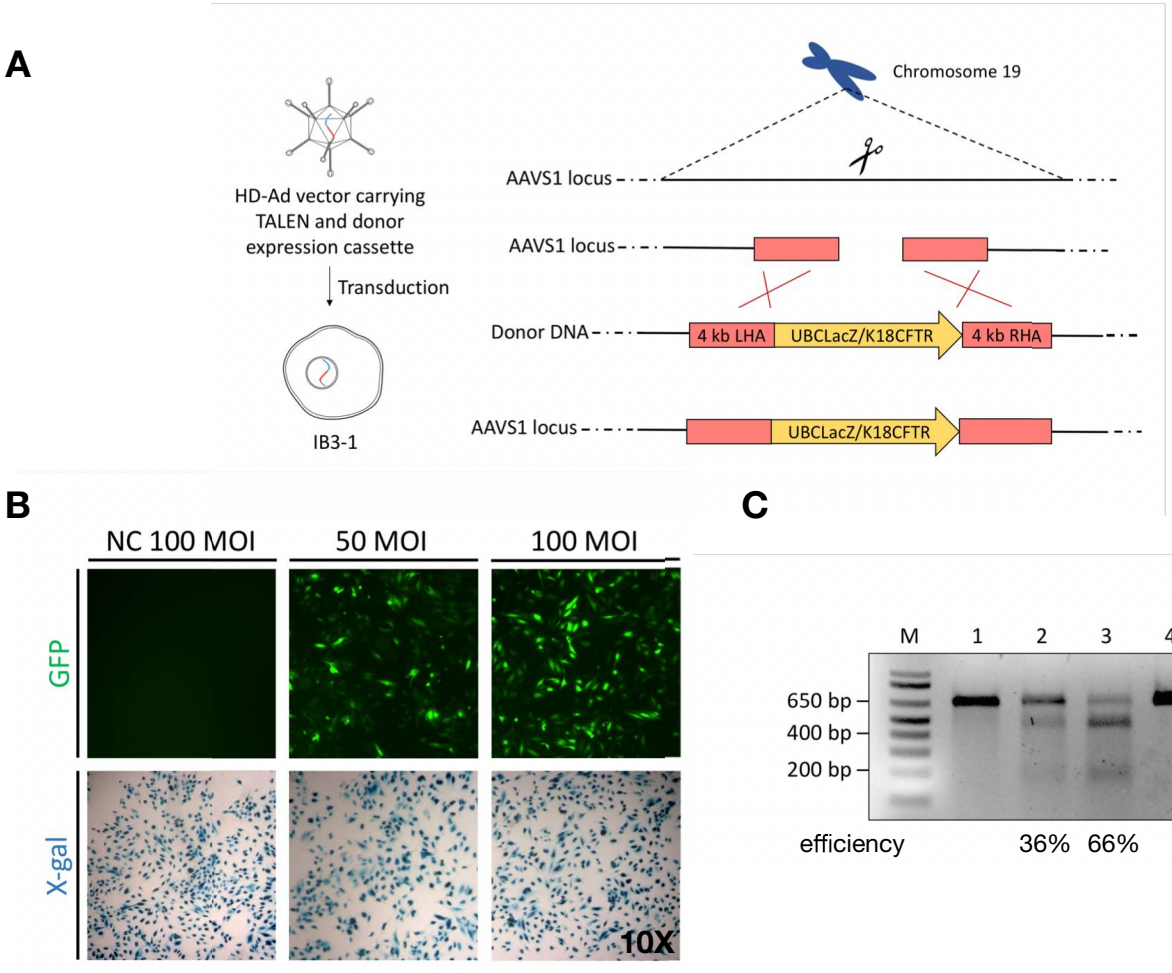

Preprints (www.preprints.org) | NOT PEER-REVIEWED | Posted: 19 November 2018 doi:10.20944/preprints201811.0444.v1

Peer-reviewed version available at Genes 2019, 10, 39; doi:10.3390/genes10010039

Figure 2

A

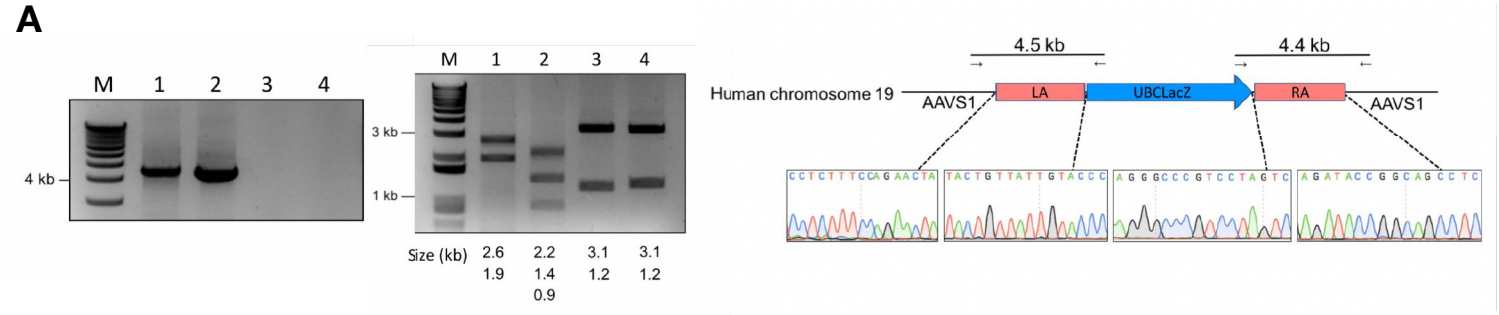

B

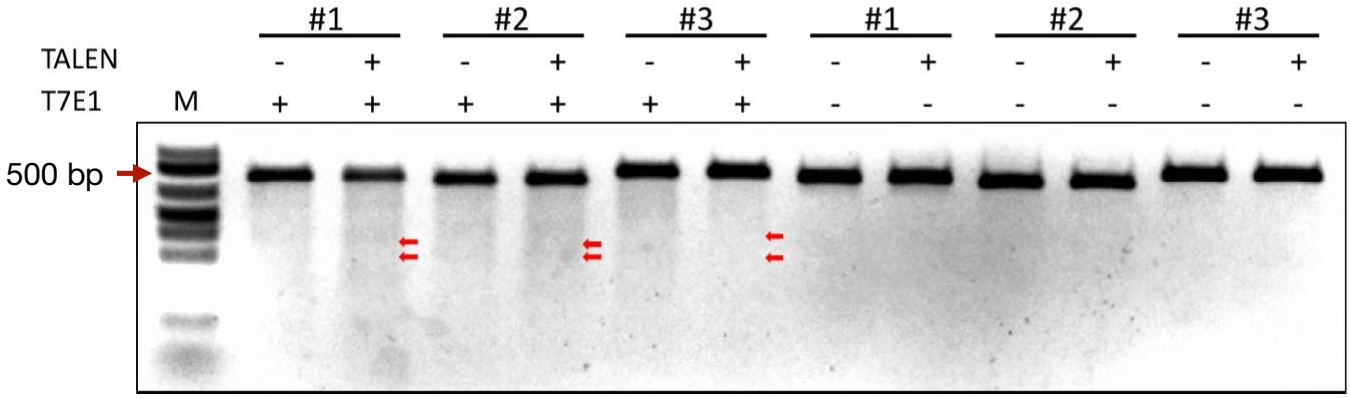

Site	Location	Exon	Full site sequence	Score
AAVS1	Chromosome 19	No	TTTTCTGTCACCAATCCTgtccctagtggccccACTGTGGGGTGGAGGGGA	0
#1	Chromosome 3	No	ATTTCTGTCAAAAATCCTtgtccactgtataagaatAGTATTAGTGAAAGACAA	-0.375
#2	Chromosome 22	No	CTCCCCCCACCCCCCAAAaaaatccatttccgggacTGGAGTGGGGACAGAAAA	-1.300
#3	Chromosome 5	No	TACTCCCCACCCCACAGAtaatctgtggtcaatgACTGTTGGATGCAGGGGA	-1.383

Peer-reviewed version available at Genes 2019, 10, 39; doi:10.3390/genes10010039

Figure 3

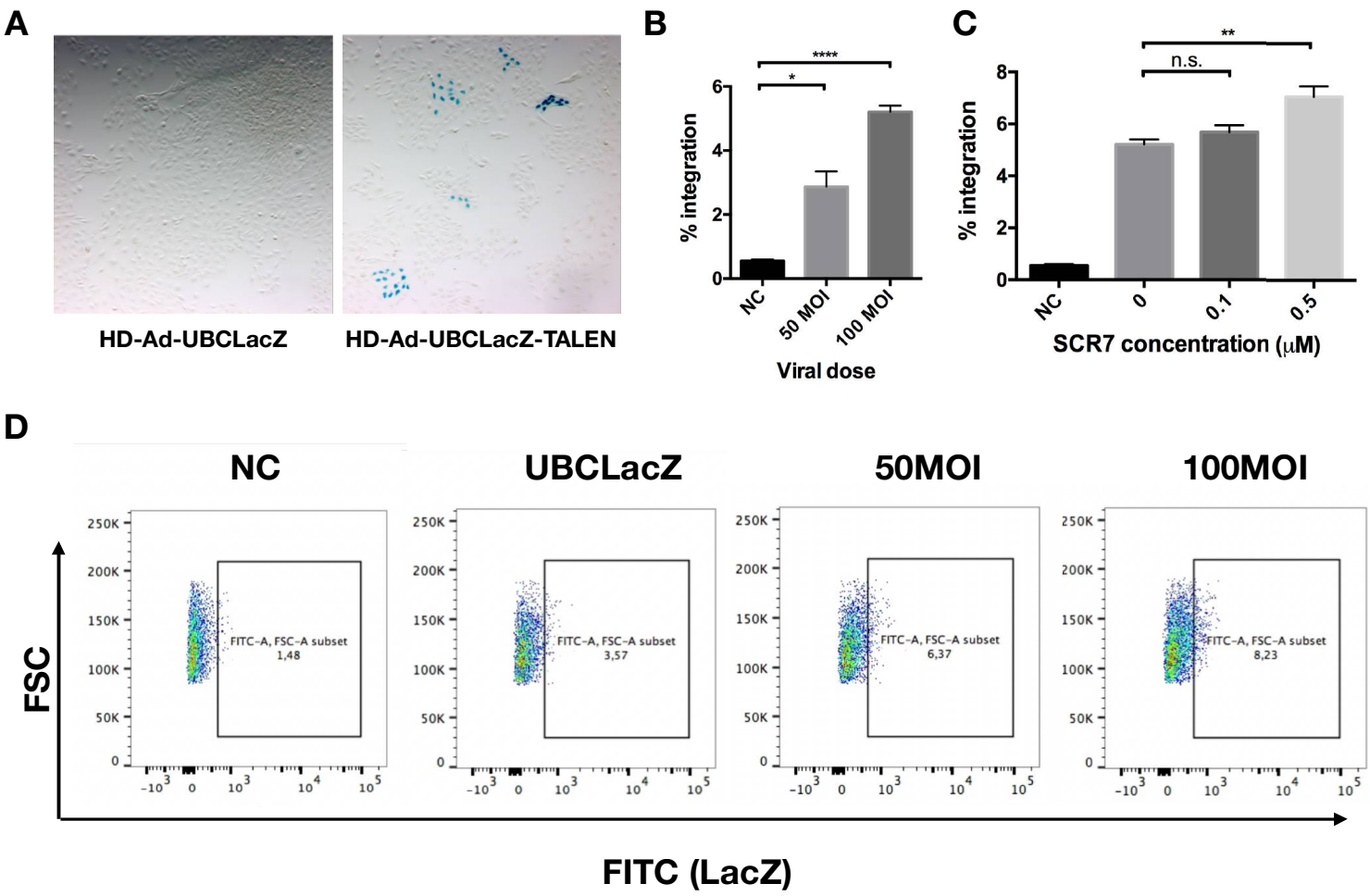

Preprints (www.preprints.org) | NOT PEER-REVIEWED | Posted: 19 November 2018 doi:10.20944/preprints201811.0444.v1

Peer-reviewed version available at *Genes* **2019**, *10*, 39; doi:10.3390/genes10010039

Figure 4

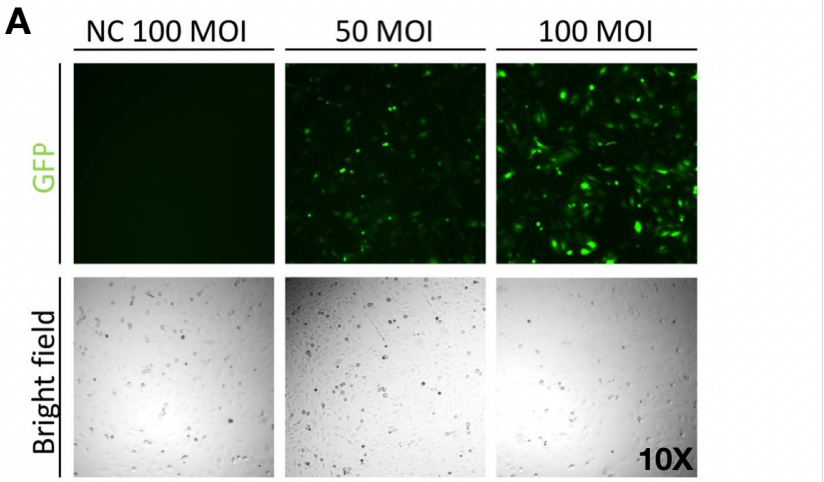

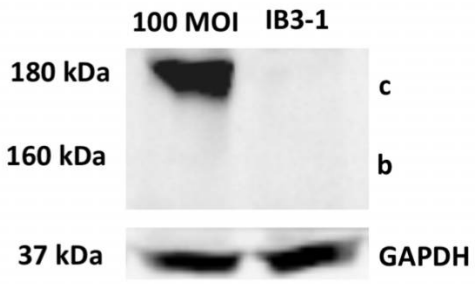

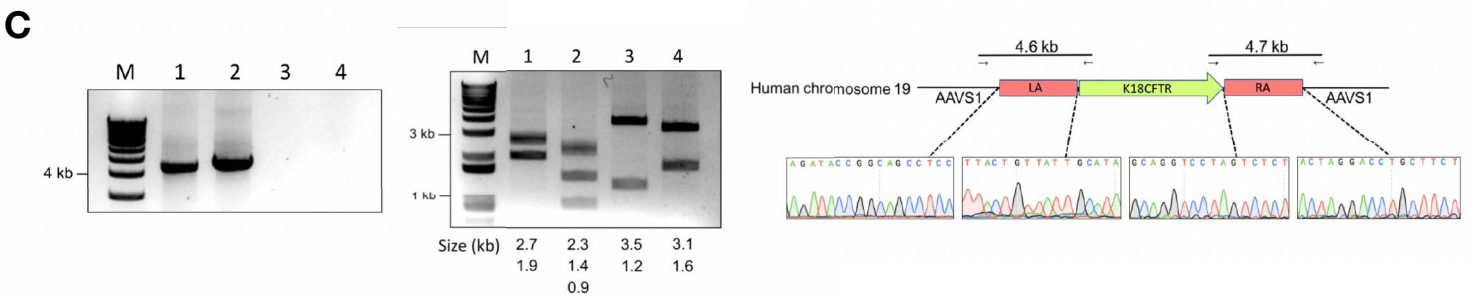

Preprints (www.preprints.org) | NOT PEER-REVIEWED | Posted: 19 November 2018 doi:10.20944/preprints201811.0444.v1

Peer-reviewed version available at Genes 2019, 10, 39; doi:10.3390/genes10010039

Figure 5

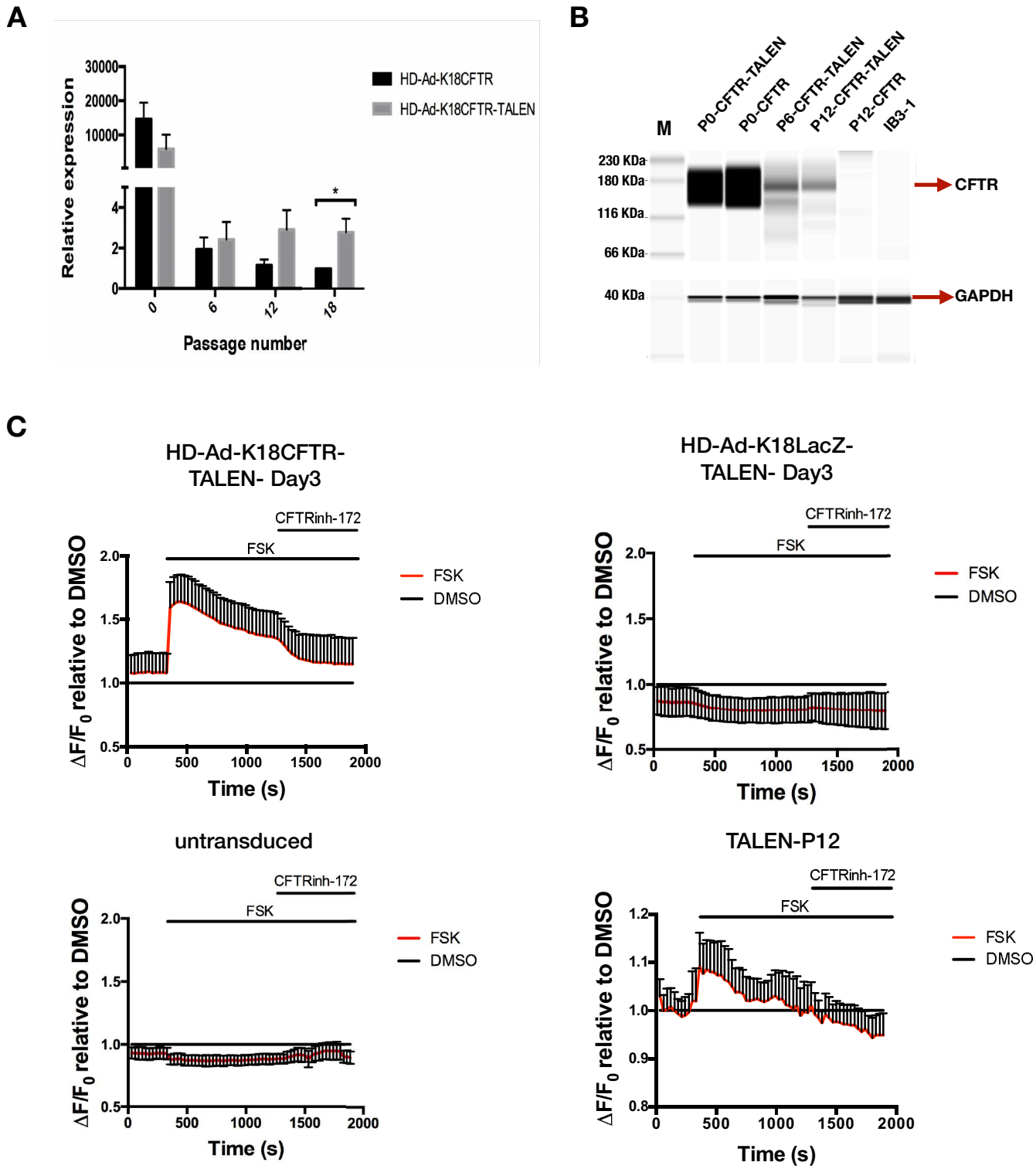

Preprints (www.preprints.org) | NOT PEER-REVIEWED | Posted: 19 November 2018 doi:10.20944/preprints201811.0444.v1

Peer-reviewed version available at Genes 2019, 10, 39; doi:10.3390/genes10010039

Figure 6